Geophys. J. Int. (2005) **162,** 755–763 doi: 10.1111/j.1365-246X.2005.02691.x

Signature of the quiet-time magnetospheric magnetic field and its electromagnetic induction in the rotating Earth

Stefan Maus[1,2] and Hermann Lühr[3]

[1] *Cooperative Institute for Research in Environmental Sciences (CIRES), University of Colorado at Boulder, Boulder, CO* 80309-0216*, USA*
[2] *National Geophysical Data Center, NOAA E/GC1,* 325 *Broadway, Boulder, CO* 80305-3328*, USA. E-mail: stefan.maus@noaa.gov*
[3] *GeoForschungsZentrum Potsdam, Telegrafenberg,* 14473 *Potsdam, Germany*

Accepted 2005 May 16. Received 2005 March 22; in original form 2004 November 24

SUMMARY

Accurate models of the magnetospheric field during magnetically quiet times are essential for high-resolution mapping of core field dynamics, mantle and ocean induction, crustal fields and ionospheric currents. Satellite data sampled at low-Earth orbit allow for a separate determination of the external contributions from currents in the magnetosphere. We have used Ørsted and CHAMP data from the years 1999–2004 to investigate this field component. In contrast to earlier studies, the field is decomposed here into contributions from sources in the solar-magnetic (SM) frame and those in the geocentric-solar-magnetospheric (GSM) frame. For an observer on the Earth, stable fields in those frames generate different diurnal and annual variations which, in response, induce currents in the subsurface. All of these effects have been modelled here. Our primary findings are: in the GSM frame, there is a dominant constant magnetic field of about 13 nT, pointing due southward. This field component is attributed to the quiet-time tail current system. The interplanetary magnetic field (IMF) contributes to the near-Earth field with 10 per cent of its Bx and about 25 per cent of its By component. For the SM frame, we obtain a constant field of 7.6 nT and a variable part which can be parametrized by the D_{ST} index. The field in SM is attributed to the combined effect of the magnetopause and ring current. A comparison of the external field variations, predicted by our satellite-derived model, with the measurements of five latitudinally distributed ground observatories shows a remarkable agreement.

Key words: electromagnetic induction, geomagnetic field, geomagnetism, magnetosphere.

1 INTRODUCTION

In high-resolution geomagnetic field modelling, a proper consideration of the field contribution coming from outside the Earth is very important and can be the limiting factor in accurately determining the various contributions to the field. The relevance of external contributions for main field modelling has been outlined, for example, by Langel *et al.* (1996). The sources for the external fields can be roughly divided into three classes. When considering a low-Earth orbiting satellite, there are magnetospheric currents flowing above the spacecraft, ionospheric currents below it and field-aligned currents connecting the two regions. In addition we have to take the induction currents in the subsurface into account, which are driven by temporal or spatial changes of the current systems in space. Here we concentrate on the magnetospheric currents and their magnetic effect close to the Earth.

It has been recognized for some time that an accurate representation of the magnetospheric field in geomagnetic field modelling requires spherical harmonic (SH) coefficients varying with multiples of annual and diurnal frequencies. Indeed, Olsen (2002) used eight static, eight annually and eight semi-annually varying coefficients as independent parameters in his OSVM series of models. The comprehensive model (Sabaka *et al.* 2002, 2004) additionally includes multiples of diurnal frequencies and uses a total of 800 independent parameters to describe a magnetospheric field to *SH* degree 2. We take a somewhat different approach. The current systems of the inner- and outer magnetosphere are treated separately. Within the inner magnetosphere, the strong geomagnetic field determines the charged particle motion and, hence, the current geometry. In the outer magnetosphere, the electrodynamics are controlled primarily by the interaction of the solar wind with the weaker geomagnetic field.

The ring current is the most prominent system in the inner magnetosphere. Since it is closely coupled to the magnetic field, it can be described quite efficiently in the solar-magnetic (SM) frame. The origin of this frame is the centre of the Earth. The *z*-axis is aligned with the geomagnetic dipole axis, pointing northward, the *x*-axis points in the direction of the Sun and *y* completes the triad. Dominant currents in the outer magnetosphere are the magnetopause surface currents and the cross-trail current. These currents are thought to

be organized in the geocentric-solar-magnetospheric (GSM) frame. The origin of that frame is again the centre of the Earth. However, the *x*-axis always points towards the Sun, the *y* axis is perpendicular to the geomagnetic dipole axis pointing eastward and *z* completes the right-handed system. The main difference between SM and GSM is that *z* is aligned with the dipole axis only in the SM frame. More details of the coordinate systems can be found in Kivelson & Russell (1995, pp. 536).

Traditionally in main field modelling, the magnetospheric field is treated in a geocentric-Earth-fixed (GEO) system (e.g. Cain 1966; Langel & Estes 1985; Olsen 2002). The derived spherical harmonic external coefficients are based on data sampled on the nightside. While the derived external magnetic field model and its parametrization produces acceptable results on the nightside, it shows clear deficits when extrapolated to the dayside. This is particularly disturbing for satellite studies of the ionospheric current systems which are strongest by far on the dayside. In view of these known shortcomings, the Comprehensive Model (Sabaka *et al.* 2002, 2004) made an important step forward by including an external field parameterization in SM. However, for the parametrization of the corresponding induced fields it was incorrectly assumed that the induction frequency is the highest frequency of the external field in SM. This implies that the Earth is stationary in SM, which is formally equivalent to the earlier assumptions of a co-rotating magnetosphere. As shown here, a correct representation of the induced fields has to account for the rotation of the Earth *against* the external fields. This is formally equivalent to a stationary Earth with the magnetosphere rotating around it.

In this study we try to distinguish between the contributions from the inner and outer magnetosphere by separating the magnetic effects which are organized, respectively, in SM and GSM frames. Diurnal and annual changes in the orientation of the SM against the GSM frame lead to different magnetic field signatures of currents organized in SM and GSM. Exploiting these differences, and including further physical considerations about the sources, we construct a simple magnetospheric field model with contributions from SM and GSM. With the help of this model, we claim that the effect of the quiet-time magnetospheric field can be predicted more reliably at all latitudes and local times. In the sections to follow we first describe the necessary theoretical tools for parametrizing GSM and SM fields, including the secondary internal fields induced by Earth rotation. Then we estimate a simple 14 parameter field model from CHAMP and Ørsted satellite data, which is finally validated on independent ground observatory measurements.

2 THEORY

The time-varying magnetospheric field, as seen by observatories and low orbiting satellites, does not, even during quiet times, average out to zero. We will refer to this time average field as the steady magnetospheric field. We expect this steady external field to be well ordered when treated by a combination of GSM and SM parameters. Constant fields in GSM and SM appear as time varying fields in GEO, as illustrated in Fig. 1. This offers the intriguing possibility to describe a significant part of the observed periodic time variations of the magnetic field by a small set of constant coefficients. In the following we discuss the properties of constant GSM and SM fields, as seen in GEO, and derive the necessary tools for estimating them, including their induction effects, from near-Earth observations.

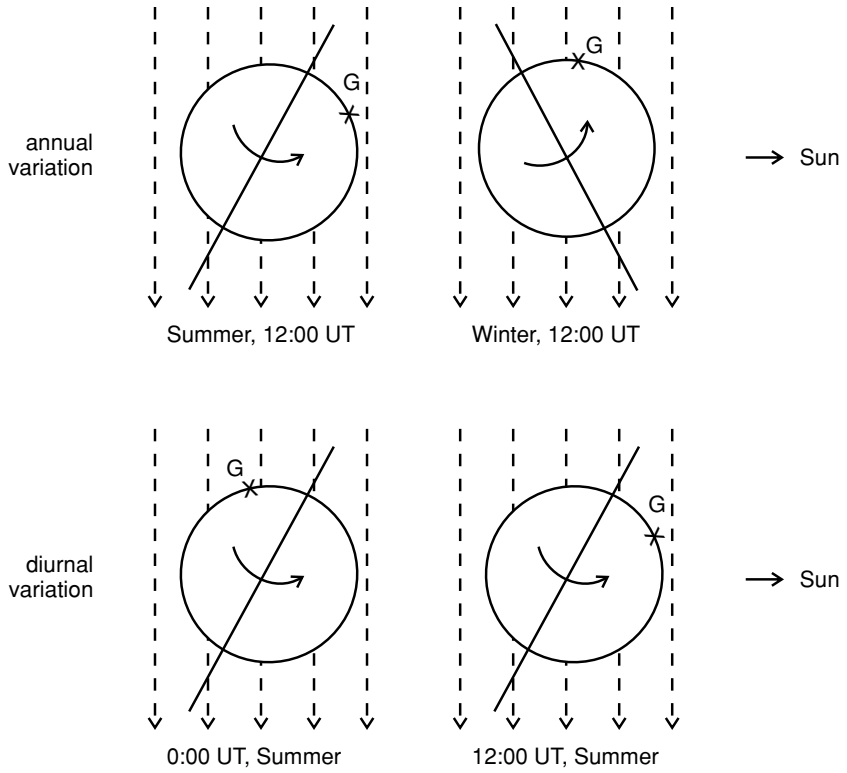

Figure 1. A stable field in the negative GSM *z* direction is seen as a seasonally and daily varying field by an Earth-fixed observer. Shown here is a projection onto the GSM *xz*-plane. An observer at Greenwich (G) sees a nearly horizontal field at noon in the summer and a nearly vertical field at noon in the winter, perceiving this as an annual variation (top row). Similarly, a nearly vertical field at midnight in summer, versus a nearly horizontal field at noon, is recorded as a daily variation (bottom row).

2.1 Spherical harmonic representation of the external field

For sources in the distant magnetosphere, the magnetic field near the Earth can be represented by the negative gradient of a scalar potential $\mathbf{B} = -\nabla V$. The potential V can be expanded into spherical harmonics (SH) as

$$V(r, \vartheta, \varphi, t) = R_E \sum_{n=1}^{N_s} \left(\frac{r}{R_E}\right)^n \sum_{m=-n}^{n} E_n^m(t) \breve{\beta}_n^m(\vartheta, \varphi), \tag{1}$$

where r, ϑ and φ are the radius, co-latitude and longitude, respectively, in the chosen Earth-centred spherical coordinate system (GEO, GSM or SM), $R_E = 6371.2$ km is the traditional geomagnetic reference radius, N_s is the spatial degree of the expansion, E_n^m are the *SH* coefficients of the external field, and $\breve{\beta}_n^m(\vartheta, \varphi)$ are Schmidt semi-normalized surface spherical harmonic functions in the convenient notation of Backus *et al.* (1996, p. 141)

$$\breve{\beta}_n^m = \cos m\phi \ \breve{P}_n^m(\cos\theta), \quad 0 \le m \le n, \tag{2}$$

$$\breve{\beta}_n^{-m} = \sin m\phi \ \breve{P}_n^m(\cos\theta), \quad 1 \le m \le n. \tag{3}$$

Here, the functions $\breve{P}_n^m(\mu)$ are defined as

$$\breve{P}_n^m(\mu) = \begin{cases} \sqrt{2\frac{(n-m)!}{(n+m)!}} P_n^m(\mu) & \text{if } 1 \le m \le n \\ P_n(\mu) & \text{if } \ m = 0, \end{cases} \tag{4}$$

where $P_n^m(\mu)$ are the associated Legendre functions (Backus *et al.* 1996, eq. 3.7.2).

2.2 Co-estimating a GSM field

If the induced field is ignored, the *SH* coefficients of an external field in GSM can be co-estimated with an *SH* expansion of the internal field in GEO, as was done for the main field model POMME-1.4 (Maus *et al.* 2005). In a linear least-squares estimation, as applicable to magnetic vector measurements, the equation

$$\boldsymbol{G}\mathbf{m} = \mathbf{d} + \mathbf{e} \tag{5}$$

is solved by

$$\mathbf{m} = (\boldsymbol{G}^T\boldsymbol{G})^{-1}\boldsymbol{G}^T\mathbf{d}, \tag{6}$$

where $\boldsymbol{G}$ is the Green tensor relating the vector of model parameters $\mathbf{m}$ (see Table 2 of the Results section as an example), to the vector of observations $\mathbf{d}$, with data errors $\mathbf{e}$. The Green tensor gives the expected effect of a unit perturbation of the model parameters on the observations. For example, if the kth datum is a measurement $Z(\mathbf{r}, t)$ of the vertical magnetic field, the entry in the ith column and kth row of the Green tensor specifies the effect $\delta Z(\mathbf{r}, t)$ at this particular location $\mathbf{r}$ and time t of a unit perturbation of the ith model parameter. Hence, to co-estimate a spherical harmonic coefficient in GSM, all one has to do is

(1) transform the location of each data point from GEO to GSM,
(2) compute the magnetic field vector for a unit perturbation of this coefficient and
(3) transform this vector back to GEO to include it in the Green tensor. The necessary coordinate transforms can be found in the space physics coordinate transforms users guide of Hapgood (1992).

The caveat of this approach is, however, that the field resulting from currents induced in the subsurface cannot be accounted for. To correctly model the field induced in the Earth due to its rotation in a constant GSM field, one has to determine the full temporal and spatial variability of the corresponding field in GEO. Interestingly, these apparent time variations in GEO result from the superposition of two different effects, discussed in the following.

2.3 Rotation in the Sun-synchronous field

To appreciate the first effect, assume that the dipole is aligned with the Earth's spin axis. Then, a constant Sun-synchronous zonal (order $m = 0$) field would appear as a constant field in GEO, whereas a field of order $m > 0$ would primarily appear as a time varying field of frequency m cpd (cycles per day) in GEO. This line of reasoning still holds when the geomagnetic dipole axis is not parallel to the spin axis, that is, for a constant field in SM coordinates. However, magnetic fields from the outer magnetosphere are better described in GSM coordinates, which adds an additional important effect, described next.

2.4 Wobble of the GSM z-axis in GEO

The geomagnetic dipole axis performs a daily rotation at an angle of about 10.5° about the Earth's spin axis. In addition, the spin axis performs an apparent annual rotation at an angle of 23.4° around the normal to the ecliptic plane, tilting towards the Sun in summer and away from it in winter. The crucial point of the GSM frame is that its z-axis follows the dipole axis only in its movements perpendicular to the Sun–Earth line. The GSM z-axis does not follow movements of the dipole axis towards and away from the Sun. This generates a wobble of the GSM z-axis in the GEO frame (in contrast to the SM z-axis which remains fixed in GEO). This wobble has a daily and an annual modulation. Therefore, a constant zonal field in GSM appears as a diurnal and annually varying field in GEO, due to the changing orientation of the GSM z-axis. The dominant frequencies of this wobble are 1 cpa (cycle per annum) and 1 cpd, but higher multiples are also required in order to accurately describe it.

2.5 Joint effect in GEO of Earth rotation and wobble of the GSM z-axis

Combining the effect of rotating within a steady GSM field of spatial degree N_s with the wobble of the GSM z-axis, we require a temporal expansion to degree $N_t \ge N_s + 1$ to describe the temporal variation of the field in GEO. This field in GEO then results as a modulation (product) of annual variations (1st factor in eq. 7, below) of frequencies $0, \ldots, N_t$ cpa with diurnal variations (2nd factor in eq. 7) of frequencies $0, \ldots, N_t$ cpd. Regarding spatial structure: The part of the field that can be described by spherical harmonics of degree n is invariant under rigid rotations (Backus *et al.* 1996, p. 59). In other words, a field of degree n in GSM remains a field of degree n in GEO. Combining these temporal and spatial considerations, one arrives at the following ansatz: A constant field of degree N_s with *SH* coefficients $E_n^{m'}$ in GSM can be represented by a time varying SH expansion in GEO of the same degree, with coefficients ϵ_n^m of all degrees n and orders m given as

$$\epsilon_n^m(t) = \sum_{m'=-n}^{n} \sum_{j=0}^{N_t} \sum_{k=0}^{N_t} \Re\left\{A_{n,m',m,j}\, e^{ij\omega_a t}\right\} \Re\left\{D_{n,m',m,k}\, e^{ik\omega_d t}\right\} E_n^{m'}, \tag{7}$$

where $\Re$ denotes the real part, $i = \sqrt{-1}$, annual frequency $\omega_a = 2\pi/a$ where a is the number of seconds in a year, diurnal frequency $\omega_d = 2\pi/d$ where d is the number of seconds in a day, and $A_{n,m',m,j}$

and $D_{n,m',m,k}$ are complex transform coefficients, with the imaginary parts of the special cases $\Im\{A_{n,m',m,0}\} = 0$ and $\Im\{D_{n,m',m,0}\} = 0$ by definition. Note that the product in (7) is between two real parts. This is because the physical realizations of the annual and diurnal variations, respectively, are given by their real parts. Multiplying the non-physical imaginary parts results in a non-physical real number. Indeed, if the real parts were not specifically taken in (7), one could combine the complex coefficients $A_{n,m',m,j}$ and $D_{n,m',m,k}$ to a single complex coefficient $C_{n,m',m,j,k}$. We have verified that (7) cannot be simplified in this way, necessitating the more complicated representation given in (8), below. The transform coefficients $A_{n,m',m,j}$ and $D_{n,m',m,k}$ could probably be derived analytically. However, this seemed a daunting task, so a numerical estimation was chosen here.

2.6 Coefficients for the transform of an *SH* expansion from GSM to GEO and from SM to GEO

For time variations of the external field with periods significantly smaller than 24 hr, the effect of Earth rotation can be ignored. For periods longer than 24 hr, and for stable external fields, one has to transform the *SH* expansion coefficients in GSM into corresponding static and time varying *SH* coefficients in GEO, the latter representing the inducing field. Estimating $A_{n,m',m,j}$ and $D_{n,m',m,k}$ in (7) is a non-linear problem. Since only the products of these coefficients are required, we estimate the matrix C of all possible permutations of real and imaginary parts of A and D, given by

$$C_{n,m',m,j,k} = \begin{cases} \Re\{A_{n,m',m,j}\}\Re\{D_{n,m',m,k}\} & \text{if } j \geq 0 \;\&\; k \geq 0, \\ \Re\{A_{n,m',m,j}\}\Im\{D_{n,m',m,|k|}\} & \text{if } j \geq 0 \;\&\; k < 0, \\ \Im\{A_{n,m',m,|j|}\}\Re\{D_{n,m',m,k}\} & \text{if } j < 0 \;\&\; k \geq 0, \\ \Im\{A_{n,m',m,|j|}\}\Im\{D_{n,m',m,|k|}\} & \text{if } j < 0 \;\&\; k < 0. \end{cases} \quad (8)$$

Here, the indices j and k for the matrix C run from $-N_t$ to N_t, while the complex coefficients A and D of ansatz (7) take only positive indices j and k. For this reason, the absolute of the index is used for A and D, whenever j or k is negative. The matrix C comprising $(2N_t + 1)^2$ coefficients per n, m', m was estimated here by the following scheme:

(1) For a given *SH* coefficient (n, m') in GSM, generate a one year time series (1-hr sampling interval) of the magnetic potential on an equal area grid in GSM.

(2) Transform the potential for every grid cell to GEO.

(3) Make a least-squares estimate of the coefficients $C_{n,m',m,j,k}$ using (7) and (8).

(4) Repeat it for all pairs (n, m') up to the desired degree N_s.

For an *SH* expansion up to spatial degree N_s and temporal degree N_t, this yields a total number n_c of transform coefficients, where

$$n_c = (2N_t + 1)^2 \sum_{\nu=1}^{N_s} (2\nu + 1)^2. \quad (9)$$

For transforms from SM to GEO one can drop the annual terms, reducing the number of coefficients by a factor $(2N_t + 1)$. Tables of the coefficients up to $N_s = 3$ and $N_t = 6$, which are generally valid for any transform from GSM to GEO and from SM to GEO, are available at *http://www.ngdc.noaa.gov/seg/geomag/gsm2geo.shtml*. Depending on the required accuracy, these coefficients must be updated after about 10 yr to reflect the slowly changing orientation of the geomagnetic dipole axis.

2.7 Induced field

An external field organized in a local-time frame induces secondary magnetic fields in the Earth. For time variations of the external field with periods significantly longer than one day, the induction is dominated by the effect of Earth rotation in a constant field (Balasis *et al.* 2004). Similarly, for external fields which are steady in GSM over years, there is a contribution due to induction at annual frequencies and multiples thereof, caused by the changing orientation of the Earth's rotation axis relative to the Sun–Earth line.

In general, a time varying external field of given degree and order induces a field with contributions to all degrees and orders. However, due to the dominant radial symmetry of the Earth, cross-coupling between different degrees and orders is small, and the difference between transfer coefficients of the same degree but different order is less than 10 per cent at the induction frequencies considered here. For the present purpose, we can therefore define simplified complex transfer functions $q_n(\omega)$, for each *SH* degree n, as

$$q_n(\omega) = \frac{\tilde{\iota}_n^m(\omega)}{\tilde{\epsilon}_n^m(\omega)}, \quad (10)$$

where $\tilde{\epsilon}_n^m$ and $\tilde{\iota}_n^m$ are the complex Fourier transforms of the external and induced fields in GEO, respectively. The values of $q_n(\omega)$ used in this study, listed in Table 1, are degree averages of transfer function coefficients computed by Jakub Velimsky from a model combining heterogeneous surface conductance (Everett *et al.* 2003; Velimski *et al.* 2003) with the 1-D conductivity model B of Utada *et al.* (2003).

The induced field, ι_n^m, of degree n and order m at a particular time, t, is then given in GEO by a summation

$$\iota_n^m(t) = \sum_{\omega} \Re\left\{q_n(\omega)\tilde{\epsilon}_n^m(\omega)\, e^{i\omega t}\right\}, \quad (11)$$

where the discrete frequencies ω are integer multiples of the annual and diurnal frequencies. Using relation (7), one can now directly write down the equation for the induced fields caused by the movement of the Earth in a stable GSM field:

For the annual induction, the daily varying terms ($k > 0$) average to zero. The non-annually varying $j = 0$ terms give no induction. Thus, the induction, α_n^m, is only due to the $k = 0$, $j > 0$ terms

$$\alpha_n^m(t) = \sum_{m'=-n}^{n} \sum_{j=1}^{N_t} \Re\left\{q_n(j\omega_a) A_{n,m',m,j}\, e^{ij\omega_a t}\right\} D_{n,m',m,0}\, E_n^{m'}, \quad (12)$$

where $\Re\{\}$ is omitted for the second term because $D_{n,m',m,0}$ is real by definition.

For the induction by multiples of daily frequencies, one has to add the annual harmonics (sum over j) to get the amplitude of the diurnal variation (right side in 13), and then multiply this combined amplitude with the individual diurnal terms. Summing over k then

Table 1. Transfer function values used in this study.

	Degree 1			Degree 2		
Period	*Re*	*Im*	Phase	*Re*	*Im*	Phase
12 month	0.128	0.089	35°	0.062	0.082	53°
6 month	0.192	0.109	30°	0.118	0.122	46°
4 month	0.231	0.102	24°	0.165	0.130	38°
24 hr	0.387	0.039	5.8°	0.433	0.073	9.6°
12 hr	0.406	0.039	5.5°	0.469	0.075	9.1°
8 hr	0.417	0.037	5.1°	0.491	0.073	8.5°

gives the combined diurnal induction δ_n^m as

$$\delta_n^m(t) = \sum_{m'=-n}^{n} \sum_{k=1}^{N_t} \Re\left\{q_n(k\omega_d) D_{n,m',m,k}\, e^{ik\omega_d t}\right\} \times \sum_{j=0}^{N_t} \Re\left\{A_{n,m',m,j}\, e^{ij\omega_a t}\right\} E_n^{m'}. \quad (13)$$

2.8 Model including external and induced field

A time-invariant external field, expanded to *SH* degree N_s in GSM, can be represented in GEO, together with the fields induced by Earth rotation, by a time varying scalar potential

$$V(r,\vartheta,\varphi,t) = \sum_{n=1}^{N_s} \sum_{m=-n}^{n} V_n^m(r,\vartheta,\varphi,t), \quad (14)$$

$$V_n^m(r,\vartheta,\varphi,t) = R_E \left[\epsilon_n^m(t) \left(\frac{r}{R_E}\right)^n + \left(\alpha_n^m(t) + \delta_n^m(t)\right) \left(\frac{R_E}{r}\right)^{n+1} \right] \breve{\beta}_n^m(\vartheta,\varphi), \quad (15)$$

where $\epsilon_n^m(t)$, $\alpha_n^m(t)$, and $\delta_n^m(t)$ are given by (7), (12) and (13), respectively. Contributions from steady fields in SM can be represented in a similar way, without the annually varying terms $\alpha_n^m(t)$. To a limited extent, contributions from GSM and SM can be co-estimated, as shown below for SH coefficients E_1^0, E_2^1 and E_2^{-1}. Where possible, physical considerations can be invoked to attribute a source term to a particular coordinate system. For example, the variable ring current is organized in SM, while the penetration of the Interplanetary magnetic field is probably better described in GSM.

3 RESULTS

We estimate a basic magnetospheric field model from CHAMP and Ørsted satellite data, taking into account stable and dynamic contributions, and the respective induction in the rotating Earth. Subsequently, the model is validated on the ground by magnetic observatory measurements from the northern and southern hemispheres.

3.1 Model parameter estimation from satellite data

We use CHAMP and Ørsted scalar and vector data from 1999 to 2004, sampled at all local times. Vector measurements are used only within $\pm 50^\circ$ magnetic latitude. Data are selected for magnetically quiet times by $|D_{ST}| < 30$ nT and Kp $\leq 1+$. At high latitudes we further demand |IMF By| < 8 nT and -2 nT $<$ IMF Bz < 6 nT, following the study on polar magnetic disturbances by Ritter *et al.* (2004). Predictions of the eight dominant solar and lunar ocean tidal magnetic fields (Maus & Kuvshinov 2004), and an internal field model (POMME-2.1) (Maus *et al.* 2005) to *SH* degree 36, including linear and quadratic secular variation, is subtracted. CHAMP data are corrected for the diamagnetic effect of the ambient plasma (Lühr *et al.* 2003). We do not subtract a model of the day time Sq current system. However, this is a source internal to the sphere of satellite observations. For data equally distributed over a sphere, internal and external fields separate well in the *SH* analysis. Thus, taking care that data are equally distributed over local times and downweighting them by their number per unit area, this internal field should not substantially contaminate the estimation of the external field coefficients.

Table 2. Model coefficients estimated from satellite data.

			Order m				
		n	0	1	−1	2	−2
SM	Stable field	1	7.57				
	Stable field	2		0.48	1.74		
	E_{ST}/I_{ST} factor	1	0.79				
GSM	Stable field	1	12.90	0.11	−0.03		
	Stable field	2	0.12	−0.40	−0.07	−0.15	0.15
	IMF correlated:						
	IMF Bx factor	1		−0.10			
	IMF By factor	1			−0.23		

The derived external field model has 14 static coefficients:

(1) a steady homogeneous field aligned with the magnetic dipole, corresponding to a degree 1, order 0 (1,0) external field in SM;

(2) two parameters, (2,1) and (2,-1), of a quadrupole field, as proposed by Balasis *et al.* (2004), describing the asymmetry of the steady ring current field;

(3) a scaling factor for the time varying disturbance field in SM, tracked by the E_{ST}/I_{ST} index (Maus & Weidelt 2004), which is a decomposition of the D_{ST} index into external and induced fields in the SM frame;

(4) eight *SH* coefficients for a steady magnetospheric field in GSM and

(5) two correlation factors with IMF Bx and By in GSM, accounting for a penetration of the horizontal part of the IMF (Lesur *et al.* 2005).

The result of the least-squares estimation for the values of these coefficients is given in Table 2. The numbers are listed separately for field contributions in SM and GSM coordinates. Due to the similarity of contributions from SM and GSM, a complete *automatic* separation of GSM and SM fields is difficult. Therefore, we have limited the free parameters in SM. Even then, the first of the quadrupole terms assumes a positive value of 0.47 in SM and an almost equal negative value of -0.40 in GSM. This is likely to be an effect of the ambiguity of the separation and the true values for these two parameters may be close to zero. The separation of all of the other parameters appears convincing. Indeed, none of the eigenvalues of the inversion is exceptionally small. All values are given in nT for Schmidt semi-normalized coefficients. A positive sign for the degree 1 order 0 (1,0) coefficients indicates a southward directed magnetic field, a positive sign for (1,1) points in the $-x$ direction (away from the Sun), and a positive sign for (1,$-$1) points in the $-$ y direction (dawnward). The constant SM field amounts to 7.6 nT and the variable part is parametrized by D_{ST} with a scaling factor of 0.79. This factor indicates that 79 per cent of the disturbance field described by the D_{ST} index has a (1,0) symmetry in SM, while 21 per cent are probably due to higher degree variations of the field. In the GSM frame we find a fairly strong field of 12.9 nT, well aligned with the z axis and also pointing southward. In this frame we estimate all of the dipole and quadrupole coefficients. Interestingly, though, none of these extra terms makes a significant contribution. This still holds true when the GSM field is expanded to SH degree 3 (not shown in Table 2). This suggests that the steady GSM field consists almost entirely of a homogeneous field in the negative (southward) GSM z direction. Finally, also the penetration of the horizontal IMF was modelled. Since GSM (1,1) points in the negative x direction and GSM (1,$-$1) in the negative y direction, the estimated correlation factors with the observed hourly averages of the IMF Bx and IMF

Table 3. Details of observatories Wingst, Mbour, Bangui, Gnangara and Port-aux-Francais, used in this study. Earlier data from PAF were not used due to a baseline shift in Z.

	WNG	MBO	BNG	GNA	PAF
Location	Germany	Senegal	Central African Rep.	Australia	Kerguelen
Latitude	53.7	14.4	4.3	−31.8	−49.4
Longitude	9.1	−17.0	18.6	116.0	70.3
Data since	1981	1989	1990	1994	1989

By mean that the penetrating field is roughly parallel to the direction of the horizontal part of the IMF field, with a stronger penetration of IMF By (23 per cent) than IMF Bx (10 per cent).

It is interesting to note that previous modellers obtained a constant external degree 1 term of the order of 20 nT (e.g. Langel & Estes 1985; Olsen 2002). If we add up the constant parts of our fields, we reach a similar value. The contribution in SM, which is the frame for the ring current, is, however, only 7.6 nT. This means that a large part of the so-called 'steady ring current field' must actually be due to other magnetospheric sources, as discussed further below.

3.2 Model validation on observatory measurements

Satellites sample the magnetic field above the active ionospheric E-region. The Birkeland current system connecting the ionosphere with the magnetosphere (Kivelson & Russell 1995, Section 13.3), passing through the region of satellite orbits, generates toroidal disturbance fields which are observed by the spacecraft, but are largely absent at ground level. Since we used satellite data from all local times and all latitudes, there is ample scope for contaminations from these additional currents. A powerful test is to compare the model results with independent ground observatory measurements.

A stable GSM field generates daily variations for Earth-fixed observers, but these are difficult to distinguish from other diurnal variations, the Sq (solar quiet) current system in particular. However, the GSM field also generates apparent annual variations when the field is sampled at a fixed local time. This local time can be chosen at night time, when the influence of ionospheric currents is smallest. Our model predicts the strongest annual variation in the northward component, X, at 0:00 LT and in the eastward component, Y, at 6:00 LT. To avoid readings from sunlit times during local summer, we sampled Y at 4:00 LT. While the field in the vertical component, Z, has a strong constant part, the annual variation in Z is much smaller, also peaking at 0:00 LT.

Five observatories were chosen at latitudes ranging from -50° to 50°, as summarized in Table 3. The choice was based on the availability of data from a previous analysis (Maus & Kuvshinov 2004), the availability of the Cartesian components X and Y (opposed to declination and horizontal intensity), the availability of a long time series of minute values, and the absence of major baseline shifts. Observatory data were selected for $|D_{ST}| < 30$ nT and Kp $\leq 1+$.

The annual variation was determined by moving a 3-yr window over the considered time interval in steps of 1 yr. A linear trend was subtracted from the data in the 3-yr window. All 1-year pieces of the resulting zero-mean time-series for all 3-yr windows were finally averaged to obtain the mean annual variation. These annual variations are plotted in Fig. 2 on top of the predictions from our external field model including the contributions from induction effects. The night-time annual variation in all of the components of the observatory measurements is indeed largely explainable by a constant magnetospheric field in GSM. When applying our selection criteria, this magnetospheric field is remarkably stable over the years. In case all data are used, however, the amplitude of the observatory annual variation shows differences in the amplitude of about 5 nT between solar maximum and minimum.

4 DISCUSSION

The quiet-time magnetospheric field can be accurately described when separated into GSM and SM frames. We have shown here that a large number of coefficients is required to represent such steady magnetospheric fields in GEO coordinates. However, these coefficients are not independent and the number of free model parameters can be reduced tremendously when the magnetospheric field is represented by a combination of magnetospheric (GSM) and SM coordinates.

We have derived a simple 14 parameter external field model with constant parts in SM and GSM, a variable part in SM parametrized by the E_{ST}/I_{ST} disturbance field index, and a variable contribution in GSM correlated with the IMF By component. For all external fields in SM and in GSM, the corresponding fields induced in the rotating Earth are fully accounted for. Considering that the external field parameters were estimated exclusively from CHAMP and Ørsted satellite data, the agreement of our model predictions with ground observatory measurements is quite remarkable.

As was mentioned in the introduction, the current systems in the outer magnetosphere are probably better organized in the GSM frame. Here we want to discuss which currents could be responsible for the observed fields. Possible candidates are the tail currents and the magnetopause currents. The magnetic field of the tail is Earthward in the northern lobe and away in the southern. This gives a southward field component at the Earth. In order to be more quantitative we made a simple model calculation to check the observed field strength. We adopted the model of Olsen (1982), shown in Fig. 3, a circularly shaped tail which is divided in the mid plane by a cross-tail current flowing from dawn to dusk. The cross-tail current is split evenly and routed back over the southern and northern lobes. This current configuration is assumed to start at a distance d from the Earth and extend into infinity. For this simple geometry, the magnetic field on the centre axis of the cross-tail current can be expressed analytically and has only a z component

$$B_z = -\frac{\mu_0 J R_T}{2\pi}\left(\frac{1}{R_T}\ln\frac{R_T+\sqrt{d^2+R_T^2}}{d}+\frac{1}{\sqrt{d^2+R_T^2}}\right), \quad (16)$$

where R_T is the radius of the tail, J is the cross-trail current density and d the distance between the Earth and the start of the tail. We applied typical numbers for the variables: $d = 10\,R_E$, $R_T = 20\,R_E$ and $J = 30$ mA m^{-1}, as can be found in Kivelson & Russell (1995, pp. 310). As a result, we obtain a field of 14 nT pointing southward. This fits nicely the number in Table 2 for the constant field in GSM. Based on this match we may assume that our constant GSM field originates from the quiet-time tail currents. The fact that the order $m = 0$ coefficient in the degree 1 term strongly dominates over the others means that the Earth lies on the symmetry plane of the tail system (Fig. 3). This suggestion is also supported by the values of the quadrupole coefficients. The first three coefficients can be interpreted as a displacement of the Earth from the symmetry centre line. Since all of them are comparably small, there is no indication of a displacement of the Earth into any direction.

The field in the SM frame we have attributed largely to the ring current in the inner magnetosphere. The field value of 7.6 nT for the quiet-time ring current seems, however, to be quite low. We can

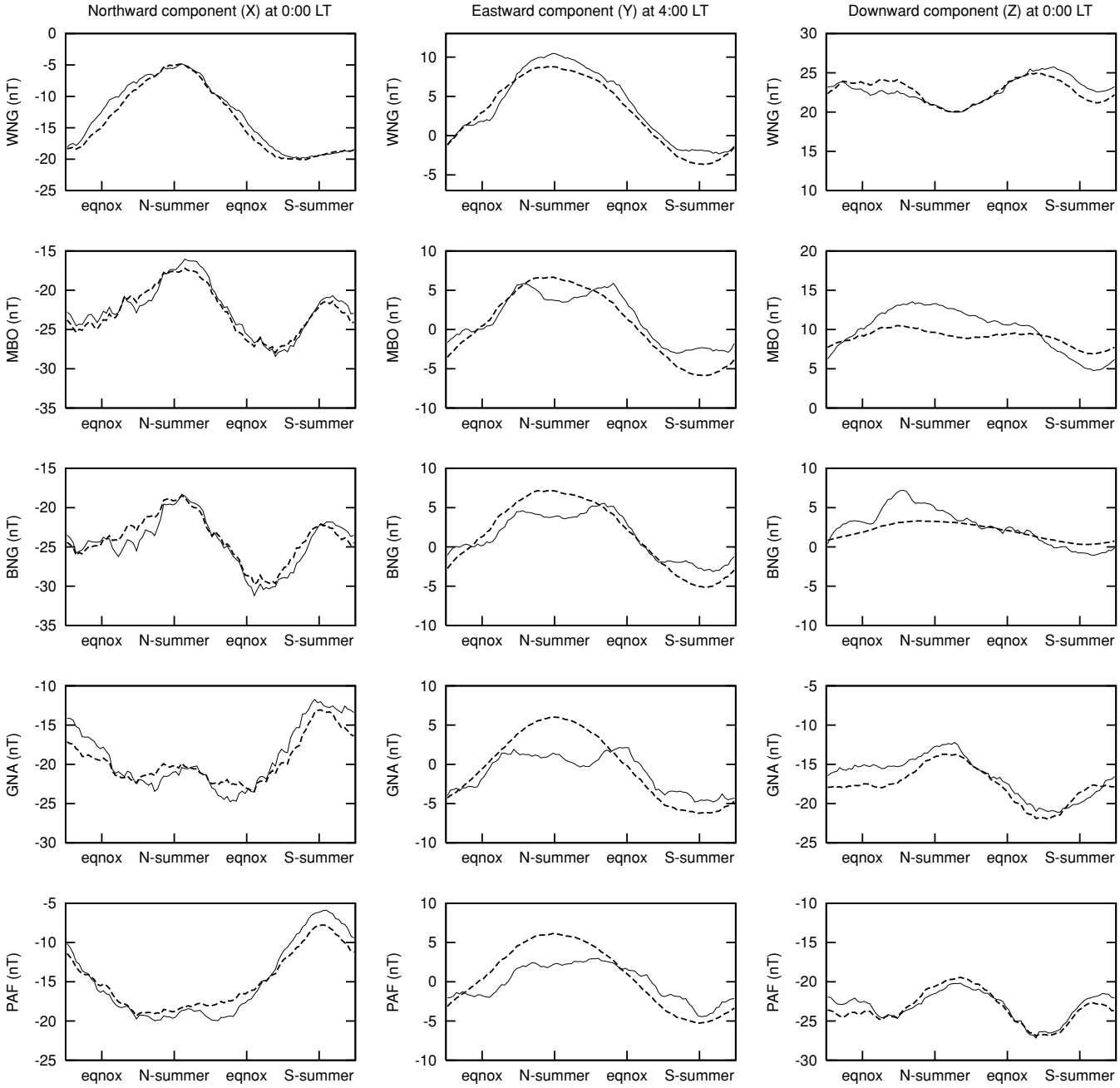

Figure 2. Night-time annual variations of the magnetic field at four observatories (see Table 3), compared with the predictions from our model (dashed line). The northernmost observatory is shown in the top row and the southernmost at the bottom. Since observatory measurements have no absolute control (due to the unknown crustal bias) constant offsets have been added to the observatory curves to shift them to the level of the model.

make use of the Parker–Dessler–Sckopke relation which relates the total energy of the charged particles carrying the ring current to the magnetic field, B_{RC}, generated at the Earth.

$$B_{RC} = -\frac{\mu_0}{2\pi}\frac{W_{\text{part}}}{B_0 R_E^3}, \tag{17}$$

where W_{part} is the total energy of the particles, B_0 the magnetic field strength at the equator and R_E the Earth radius. The minus sign indicates that the B-field is directed southward. Estimates of the ring current energy content can be derived from the measurements on board the AMPTE/CCE spacecraft. A typical number for the quiet- time ring current is $W_{\text{part}} = 1 \times 10^{15} J$ (Hamilton *et al.* 1988). Inserting this value into eq. (13) results in a ring current field of $B_{RC} = 27$ nT. This is much larger than the value we obtained in the SM frame. So far we have, however, not considered the dayside magnetopause current. When assuming a magnetopause stand-off distance of 11 R_E the estimated effect of the Chapman–Ferraro currents, B_{CF}, is 22 nT. The direction of this field is northward. When superposing both fields we obtain 5 nT southward, which is close to our constant field in SM. This result suggests that the magnetic field of the Chapman–Ferraro currents is better organized in SM than in GSM. This conclusion is also supported by the fact that all changes of the ring current plus Chapman–Ferraro current, as monitored by the D_{ST} index, can well be accounted for in the SM frame.

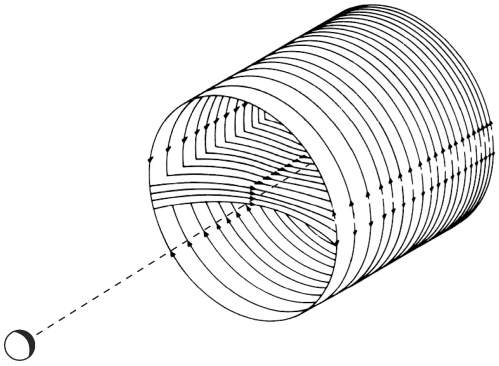

Figure 3. A simple model of the tail currents with the Earth on the centre line (dashed) in the ecliptic symmetry plane. (After Olsen 1982).

The quadrupole term $(2, -1)$ in SM can be regarded as significant. It represents a local time dependence of the ring current intensity, with stronger fields on the dusk side compared to the dawn side. This effect has been reported earlier by Langel *et al.* (1996) and has also been considered in induction studies (Balasis *et al.* 2004).

The annual variation of the observatory night-time values was observed already earlier. Campbell (1984) made use of the observatories in the American sector and constructed a global model for the expected seasonal baseline variations. Several of the features predicted by his model are in good agreement, for example, an annual variation of the horizontal components with an amplitude of up to 6 nT and the dominance of the semi-annual variation close to the equator. His variations of the Z component, on the other hand, have little in common with our results. Campbell (1984) constructed also an equivalent current system in the ionosphere, which could be responsible for the field variations on the ground. Such a system has, however, little resemblance with the real current distribution. The validity of that model is, therefore, limited to the surface of the Earth and not applicable in space.

5 CONCLUSIONS

We have presented an approach for describing the quiet-time magnetospheric field contributions in appropriate coordinate systems. This helps to minimize the number of required parameters. A number of interesting results emerged from this study concerning the signals on the ground and the current systems in the magnetosphere.

(1) A constant field of about 13 nT in the GSM frame causes diurnal and annual variations on the Earth, which amount, together with the induction effects, to about 6 nT.

(2) Magnetospheric tail currents have been identified as the main source for the GSM field.

(3) The fractions of the IMF horizontal components penetrating into the magnetosphere amount to about 25 per cent for the By component and 10 per cent for the Bx component.

(4) The ring current is well described in the SM frame. There is some indication of a local time dependence of this current, suggesting an asymmetric ring current centred around the late evening hours during quiet times.

(5) The Chapman-Ferraro currents on the magnetopause seem to be better ordered in the SM frame than in GSM.

(6) The remarkable agreement of the annual variation estimated by our approach with average night-time values of the observatories provides confidence in the obtained results.

Coefficients and software for transforming a spherical harmonic expansion from GSM or SM to GEO are available at *http://www.ngdc.noaa.gov/seg/geomag/gsm2geo.shtml*.

ACKNOWLEDGMENTS

Discussions with Gary Egbert on the induction effect of Earth rotation are gratefully acknowledged. We thank Jakub Velimsky, Mark Everett and a further referee for detailed comments and suggestions. Jakub kindly supplied the improved transfer function coefficients for an Earth model including a heterogeneous surface layer. We acknowledge the use of observatory data from Wingst (GeoForschungsZentrum), Bangui and Mbour (Institut Francais de Recherche Scientifique pour le Developpement en Cooperation), Gnangara (Geoscience Australia) and Port-aux-Francais (Ecole et Observatoire des Sciences de la Terre). Further, we acknowledge the operational support of the CHAMP mission by the German Aerospace Center (DLR) and the financial support for the data processing by the Federal Ministry of Education and Research (BMBF). The Ørsted mission is operated by the Danish Meteorological Institute, supported by the Danish Space Research Institute and the Ministries of Trade, Research and Transport.

REFERENCES

Backus, G., Parker, R.L. & Constable, C., 1996. *Foundations of Geomagnetism*, Cambridge Univ. Press, Cambridge, UK.

Balasis, G., Egbert, G. & Maus, S., 2004. Local time effects in satellite estimates of electromagnetic induction transfer functions, *Geophys. Res. Lett.,* **31,** L16610, doi:10.1029/2004GL020147.

Cain, J.C., 1966. Model of the earth's magnetic field, in *Radiation trapped in the Earth's magnetic field*, pp. 7–25, ed. McCormac, B.M., D. Reidel Publ. Co., Dordrecht, the Netherlands.

Campbell, W.H., 1984. An external current representation of the quiet nightside geomagnetic field level changes, *J. Geomag. Geoelectr.,* **36,** 257–265.

Everett, M.E., Constable, S. & Constable, C.G., 2003. Effects of near-surface conductance on global satellite induction responses, *GJI,* **153,** 277–286.

Hamilton, D.C., Gloekler, G., Ipavich, F.M., Stüdemann, W., Wilken, B. & Kremser, G., 1988. Ring current development during the great geomagnetic storm of February 1986, *J. geophys. Res.,* **93,** 14 343–14 355.

Hapgood, M.A., 1992. Space physics coordinate transformations: a user guide, *Planet. Space Sci.,* **40,** 711–717.

Kivelson, M.G. & Russell, C., (eds.), 1995. *Introduction to Space Physics*, Cambridge Univ. Press, Cambridge, UK.

Langel, R.A. & Estes, R.H., 1985. Large-scale, near-earth magnetic fields from external sources and the corresponding induced internal field, *J. geophys. Res,* **90,** 2497–2494.

Langel, R.A., Sabaka, T.J., Baldwin, R.T. & Conrad, J.A., 1996. The near-earth magnetic field from magnetospheric and quiet-day ionospheric sources and how it is modelled, *Phys. Earth planet. Int.,* **98,** 235–267.

Lesur, V., Macmillan, S. & Thomson, A., 2005. A magnetic field model with daily variations of the magnetospheric field and its induced counterpart in 2001, *Geophys. J. Int.*, **160,** 79–88.

Lühr, H., Rother, M., Maus, S., Mai, W. & Cooke, D., 2003. The diamagnetic effect of the equatorial Appleton anomaly: Its characteristics and impact on geomagnetic field modeling, *Geophys. Res. Lett.,* **30**(17), 1906, doi:10.1029/2003GL017407.

Maus, S. & Kuvshinov, A.V., 2004. Ocean tidal signals in observatory and satellite magnetic measurements, *Geophys. Res. Lett.,* **31,** L15313, doi:10.1029/2004GL020090.

Maus, S. & Weidelt, P., 2004. Separating the magnetospheric disturbance magnetic field into external and transient internal contributions using a 1D conductivity model of the earth, *Geophys. Res. Lett.,* **31,** L12614, doi:10.1029/2004GL020232.

Maus, S., Lühr, H., Balasis, G., Rother, M. & Mandea, M., 2005. Introducing POMME, Potsdam Magnetic Model of the Earth, in *Earth Observation with CHAMP: results from Three Years in Orbit*, pp. 293–298, eds. Reigber, C., Lühr, H., Schwintzer, P. & Wickert, J., Springer, Berlin—Heidelberg.

Olsen, P.W., 1982. The geomagnetic field and its extension into space, *Adv. Space Res.,* **2**(1), 13–17.

Olsen, N., 2002. A model of the geomagnetic main field and its secular variation for epoch 2000 estimated from Ørsted data, *Geophys. J. Int.,* **149,** 454–462.

Ritter, P., Lühr, H., Viljanen, A. & Maus, S., 2004. High-latitude ionospheric currents during very quiet times: their characteristics and predictability, *Ann. Geophys.,* **22,** 2001–2014.

Sabaka, T.J., Olsen, N. & Langel, R.A., 2002. A comprehensive model of the quiet-time, near-Earth magnetic field: phase 3, *Geophys. J. Int.,* **151,** 32–68.

Sabaka, T.J., Olsen, N. & Purucker, M.E., 2004. Extending comprehensive models of the Earth's magnetic field with ørsted and CHAMP data, *Geophys. J. Int.,* **159,** 521–547.

Utada, H., Koyama, T., Shimizu, H. & Chave, A.D., 2003. A semi-global reference model for electrical conductivity in the mid-mantle beneath the north Pacific region, *Geophys. Res. Lett.,* **30,** doi:10.1029/2002GL016092.

Velimski, J., Everett, M.E. & Martinec, Z., 2003. The transient Dst electromagnetic induction signal at satellite altitudes for a realistic 3D electrical conductivity in the crust and mantle, *Geophys. Res. Lett.,* **30,** doi:10.1029/2002GL016671.

Geophys. J. Int. (2005) **162,** 764 doi: 10.1111/j.1365-246X.2005.02751.x

Corrigendum

Maus, S. & Lühr, H., 2005. Signature of the quiet-time magnetospheric magnetic field and its electromagnetic induction in the rotating Earth (*Geophys. J. Int.*, **162,** 755–763)

In Maus & Lühr (2005) we were under the incorrect impression that eq. (29) of Sabaka, Olsen & Langel (2002) provided a magnetospheric field representation and its induced counterparts in solar magnetic (SM) coordinates, while this equation is in fact given in Earth-fixed coordinates. Contrary to the statement in our introduction, the induced fields are therefore correctly related to their external sources in the Comprehensive Model.

REFERENCES

Maus, S. & Lühr, H., 2005. Signature of the quiet-time magnetospheric magnetic field and its electromagnetic induction in the rotating Earth, *Geophys. J. Int.,* **162,** 755–763.

Sabaka, T.J., Olsen, N., Langel, R.A., 2002. A comprehensive model of the quiet-time, near-Earth magnetic field: phase 3, *Geophys. J. Int.,* **151,** 32–68.